J. Phys. Earth, **35**, 347–365, 1987

SUPERSHEAR ACCELERATIONS AND MACH-WAVES FROM A RUPTURING FRONT PART I. THEORETICAL MODEL AND IMPLICATIONS

Ari BEN-MENAHEM and Sarva Jit SINGH*

Department of Applied Mathematics, Weizmann Institute of Science, Rehovot 76100, Israel

(Received March 31, 1987; Revised November 24, 1987)

Acceleration fields in 3-D elastic media due to a propagating rupture at constant super-shear velocities are evaluated. The elastodynamic Green's tensor and its gradient are obtained in closed-form for arbitrary compressional and shear Mach-numbers and arbitrary source time-function. It is found that the acceleration field consists of three main phases: a Mach-wave, a starting phase, and a stopping phase. The stationary phase approximation is used to obtain the explicit dependence of the Mach-wave peak amplitude on the source, propagation, and media elements. It is shown that the Mach-wave plays a dominant role in the acceleration signal of the near-field zone.

1. *Introduction*

Observations and data analyses of ground accelerations in the near-field region of earthquake faults suggest that high local accelerations may be due to Mach-waves produced by ruptures propagating with supershear velocities (MURRAY, 1973; ARCHULETA, 1984). Moreover, observations of high-frequency near-field displacements, velocities and accelerations disclose that the near-field motion is governed by irregularities of the slip-function and that localized details rather than global averages are responsible for the peak accelerations and velocities in the near-field (CLOUD and PEREZ, 1971; DAS and AKI, 1977).

Theoretical simulations of realistic earthquake sources can be grouped into a number of categories. BEN-MENAHEM (1961) promoted 3-D kinematic propagating fault models in which the source is represented as a superposition of point dislocations. A dislocation segment begins to move at a constant subshear velocity V at $t=0$ and stops at a finite distance L from the point of rupture initiation. While moving, it separates the area of the fault surface which has slipped from that which has not. An approximation for the far supersonic radiation field was given by

* On leave from the Department of Mathematics, Maharshi Dayanand University, Rohtak 124001, India

SAVAGE (1971). EASON *et al.* (1956) obtained explicit expressions for the displacements due to a single localized force moving with a subshear velocity in a 3-D elastic medium. PAYTON (1963) generalized Eason's solution for a source that starts at a given time and derived the field for arbitrary Mach-numbers. Two-dimensional plain-strain problems with a fixed subshear source-velocity were discussed by FRANK (1949), ESHELBY (1949), and BURRIDGE (1973).

A different approach, based upon dynamical fracture mechanics, was applied to earthquake fault models by MADARIAGA (1983). The basic idea here is that the radiation of high-frequency waves is controlled by the motion of the slip-velocity concentrations.

In the present paper, we blend a new source model which is a hybrid of the above models. Consequently, we employ a kinematic source regime in which the ensuing radiation field is governed by the source's slip velocity rather than the slip itself.

In our analysis we found it more convenient to solve the inhomogeneous Navier vector equation with an appropriate moving-source term. We derive closed-form expressions for the accelerations, inside and outside the shear and compressional Mach-cones for an arbitrary source time-function.

We discuss in detail the special case of a finite line source which starts and stops and show that the acceleration field is composed of three main waves: the starting phase, the stopping phase, and the Mach-wave. The stationary phase approximation is used to obtain the explicit dependence of the Mach-wave peak amplitude upon the source, propagation, and the media elements.

2. *The Elastodynamic Green's Tensor in the Time Domain*

Consider a concentrated force in a homogeneous, isotropic, unbounded, elastic medium, acting in the direction of the unit force $\boldsymbol{a}$ and moving along the x-axis with a uniform velocity V. The ensuing displacement field is a solution of the equation

$$\alpha^2 \operatorname{grad} \operatorname{div} \boldsymbol{u} - \beta^2 \operatorname{curl} \operatorname{curl} \boldsymbol{u} - \frac{\partial^2 \boldsymbol{u}}{\partial t^2} = -\frac{\boldsymbol{a}}{\rho} Q(t)\delta(x - Vt)\delta(y)\delta(z), \tag{2.1}$$

where α, β are the intrinsic wave velocities of the medium, ρ is the mass density and $Q(t)$ is the source time-function. In order to solve Eq. (2.1), we decompose both the displacement field and the source term into their irrotational and solenoidal parts in the form (BEN-MENAHEM and SINGH, 1981; p. 152)

$$\begin{aligned} \boldsymbol{u} &= \operatorname{grad} \operatorname{div}(\boldsymbol{a}F_\alpha) - \operatorname{curl} \operatorname{curl}(\boldsymbol{a}F_\beta) \\ &= \operatorname{grad} \operatorname{div}[\boldsymbol{a}(F_\alpha - F_\beta)] + \nabla^2(\boldsymbol{a}F_\beta), \end{aligned} \tag{2.2}$$

$$-\boldsymbol{a}\delta(x - Vt)\delta(y)\delta(z) = \operatorname{grad} \operatorname{div}\left(\frac{\boldsymbol{a}}{4\pi D}\right) - \operatorname{curl} \operatorname{curl}\left(\frac{\boldsymbol{a}}{4\pi D}\right), \tag{2.3}$$

where

$$D(r, t)=[(x-Vt)^2+y^2+z^2]^{1/2}.$$

Using the representations (2.2) and (2.3), we find that Eq. (2.1) is identically satisfied if the potentials F_c $(c=\alpha, \beta)$ satisfy

$$\nabla^2 F_c-\frac{1}{c^2}\frac{\partial^2 F_c}{\partial t^2}=\frac{Q(t)}{4\pi\rho c^2 D(r, t)}. \tag{2.4}$$

Defining the Fourier transforms

$$f_c(r, \omega)=\int_{-\infty}^{\infty} F_c(r, t)e^{-i\omega t}dt, \qquad F_c(r, t)=\frac{1}{2\pi}\int_{-\infty}^{\infty} f_c(r, \omega)e^{i\omega t}d\omega, \tag{2.5}$$

$$q(\omega)=\int_{-\infty}^{\infty} Q(t)e^{-i\omega t}dt, \qquad Q(t)=\frac{1}{2\pi}\int_{-\infty}^{\infty} q(\omega)e^{i\omega t}d\omega, \tag{2.6}$$

Eq. (2.4) yields

$$(\nabla^2+k_c^2)f_c=k_c^2 s, \tag{2.7}$$

where $k_c=\omega/c$ and

$$s(r, \omega)=\frac{1}{4\pi\rho\omega^2}\int_{-\infty}^{\infty}\frac{Q(t)}{D(r, t)}e^{-i\omega t}dt. \tag{2.8}$$

We note that

$$\nabla^2\frac{1}{D(r, t)}=-4\pi\delta(x-Vt)\delta(y)\delta(z), \tag{2.9}$$

$$(\nabla^2+k_c^2)\left[\frac{e^{-ik_c D(r,t)}}{D(r, t)}\right]=-4\pi\delta(x-Vt)\delta(y)\delta(z). \tag{2.10}$$

Putting

$$f_c(r, \omega)=\chi(r, \omega)+s(r, \omega), \tag{2.11}$$

Eqs. (2.7) to (2.9) show that $\chi(r, \omega)$ satisfies the equation

$$(\nabla^2+k_c^2)\chi=-\nabla^2 s=\frac{1}{\rho\omega^2}\int_{-\infty}^{\infty} Q(t)\delta(x-Vt)e^{-i\omega t}dt\,\delta(y)\delta(z). \tag{2.12}$$

Equation (2.10) now reveals that a particular solution of Eq. (2.12) is

$$\chi(r, \omega)=-\frac{1}{4\pi\rho\omega^2}\int_{-\infty}^{\infty}\frac{Q(t)}{D(r, t)}e^{-ik_c D(r,t)-i\omega t}dt. \tag{2.13}$$

From Eqs. (2.8), (2.11), and (2.13), we have

$$f_c(r,\omega)=\frac{1}{4\pi\rho\omega^2}\int_{-\infty}^{\infty}\frac{Q(t')}{D(r,t')}[1-e^{-ik_cD(r,t')}]e^{-i\omega t'}dt'. \tag{2.14}$$

Applying the inverse Fourier transform [Eq. (2.5)] to Eq. (2.14), we obtain

$$F_c(r,t)=\frac{1}{8\pi^2\rho}\int_{-\infty}^{t}\frac{Q(t')}{D(r,t')}dt'\int_{-\infty}^{\infty}\frac{1}{\omega^2}[1-e^{-i(\omega/c)D(r,t')}]e^{i\omega(t-t')}d\omega. \tag{2.15}$$

With the help of Eq. (2.15), we can recast Eq. (2.2) in the form

$$\boldsymbol{u}(\boldsymbol{r},t)=\vec{G}(\boldsymbol{r},t)\cdot\boldsymbol{a}, \tag{2.16}$$

where the Green's tensor $\vec{G}$ is given by

$$\vec{G}(\boldsymbol{r},t)=\frac{1}{4\pi\rho}\nabla\nabla\Theta+\frac{\vec{I}}{4\pi\mu}S_\beta, \tag{2.17}$$

$$\Theta=\frac{1}{2\pi}\int_{-\infty}^{t}\frac{Q(t')}{D(r,t')}dt'\int_{-\infty}^{\infty}\frac{1}{\omega^2}[e^{-i(\omega/\beta)D(r,t')}-e^{-i(\omega/\alpha)D(r,t')}]e^{i\omega(t-t')}d\omega, \tag{2.18}$$

$\vec{I}$ is the unit tensor, and S_β is given in Eq. (2.21).

The spectral counterpart of Eq. (2.17) is

$$\begin{aligned}\vec{G}(\boldsymbol{r},\omega)=&\frac{\vec{I}}{4\pi\mu}\int_{-\infty}^{\infty}\frac{Q(t')}{D(t')}e^{-i\omega(t'+D/\beta)}dt'\\&+\frac{1}{4\pi\rho\omega^2}\nabla\nabla\left[\int_{-\infty}^{\infty}\frac{Q(t')}{D(t')}(e^{-i\omega D/\beta}-e^{-i\omega D/\alpha})e^{-i\omega t'}dt'\right].\end{aligned} \tag{2.19}$$

For the determination of the acceleration field $\ddot{\boldsymbol{u}}(t)$, it is essential to calculate the second time-derivative of $\vec{G}$. From Eq. (2.17)

$$\ddot{\vec{G}}(\boldsymbol{r},t)=\frac{\vec{I}}{4\pi\mu}\ddot{S}_\beta-\frac{1}{4\pi\rho}\nabla\nabla(S_\beta-S_\alpha), \tag{2.20}$$

where

$$S_c=\int_{-\infty}^{t}\frac{Q(t')}{D(t')}\delta\left(t-t'-\frac{D}{c}\right)dt',\qquad c=\alpha,\beta \tag{2.21}$$

$$D(t')=[(x-vt')^2+\Delta^2]^{1/2},\qquad \Delta^2=y^2+z^2.$$

Explicitly,

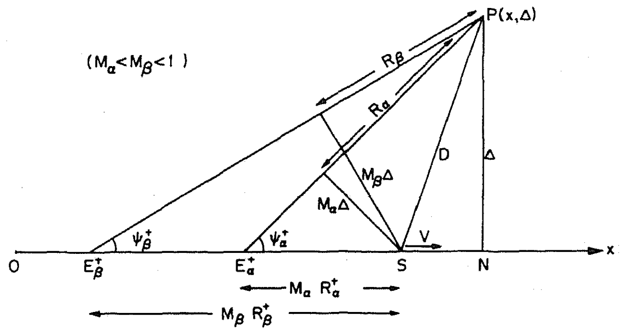

Fig. 1. A seismic source in subshear motion. The location of the observer is arbitrary. The observer at P receives at time t, a shear wave which was emitted by the source when it was at the point E_β^+ at time t_β^+ and a compressional wave which was emitted by the source when it was at the point E_α^+ at time t_α^+. Note that since $R_\alpha > R_\beta$, we have $\psi_\alpha^+ > \psi_\beta^+$.

$$S_c(r, t) = \int_{-\infty}^{t} \frac{Q(t')}{D(t')} \delta\left(t - t' - \frac{D}{c}\right) \mathrm{d}t'$$

$$= \begin{cases} \dfrac{1}{R_c} Q\left(t - \dfrac{R_c^+}{c}\right) & \text{for} \quad M_c < 1 \\[2ex] \dfrac{\dot{1}}{ct - x} Q\left(t - \dfrac{R_c^0}{c}\right) & \text{for} \quad M_c = 1 \\[2ex] \dfrac{1}{R_c} Q\left(t - \dfrac{R_c^+}{c}\right) + \dfrac{1}{R_c} Q\left(t - \dfrac{R_c^-}{c}\right) & \text{for} \quad M_c > 1\,, \end{cases} \tag{2.22}$$

where

$$R_c^{\pm} = \frac{1}{1 - M_c^2} [M_c(x - Vt) \pm R_c]\,,$$
$$R_c = [(x - Vt)^2 + (1 - M_c^2)\Delta^2]^{1/2}\,, \tag{2.23}$$
$$R_c^0 = \frac{(ct - x)^2 + \Delta^2}{2(ct - x)}\,.$$

It may be noted that

$$S_c = 4\pi\rho c^2 V^2 F_c\,.$$

We now have two Mach-numbers, $M_\alpha = V/\alpha$ and $M_\beta = V/\beta$. Thus, five distinct cases arise, depending upon the value of V. These are:

I. $M_\alpha < M_\beta < 1$,
II. $M_\alpha < M_\beta = 1$,
III. $M_\alpha < 1 < M_\beta$,

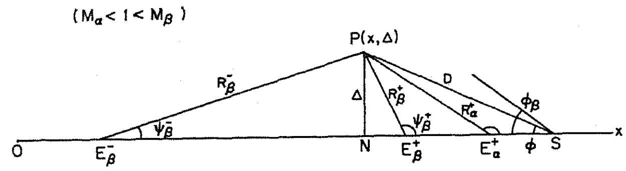

Fig. 2. A seismic source in supershear-subcompressional motion. When the point P lies inside the shear Mach-cone, i.e., when $\phi < \phi_\beta = \sin^{-1}(1/M_\beta)$, two shear waves and a compressional wave are simultaneously received at it. However, if P lies outside the shear Mach-cone, only the compressional wave is received.

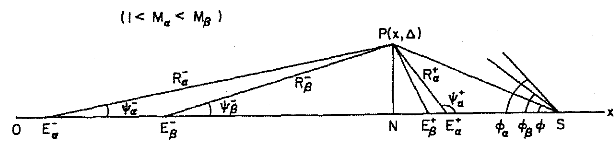

Fig. 3. A seismic source in supercompressional motion. When $\phi < \phi_\beta = \sin^{-1}(1/M_\beta)$, two shear and two compressional waves are simultaneously received at P. When $\phi_\beta = \sin^{-1}(1/M_\beta) < \phi < \phi_\alpha = \sin^{-1}(1/M_\alpha)$, only two compressional waves are received. Note that $\psi_\alpha^- < \psi_\beta^-$.

IV. $M_\alpha = 1 < M_\beta$,
V. $1 < M_\alpha < M_\beta$.

The geometry of the subshear motion ($M_\beta < 1$) is depicted in Fig. 1. Since $M_\alpha < M_\beta$ it is clear from Eq. (2.17) that $R_\alpha > R_\beta$. Two waves are simultaneously received at the point P; one shear wave emitted by the source at time $t - \tau_\beta^+$ (see list of symbols) when it was at E_β^+ and the other a compressional wave emitted by the source at time $t - \tau_\alpha^+$ when it was at E_α^+. The time for the shear wave from E_β^+ to P is τ_β^+ and the time for the compressional wave from E_α^+ to P is τ_α^+.

The geometry of the supershear-subcompressional motion ($M_\alpha < 1 < M_\beta$) is given in Fig. 2. A point P inside the shear Mach-cone $[\phi < \phi_\beta = \sin^{-1}(1/M_\beta)]$ receives simultaneously three waves: a shear wave emitted at time $t - \tau_\beta^-$ when the source was at E_β^-, another shear wave emitted at time $t - \tau_\beta^+$ when the source was at E_β^+, and a compressional wave emitted at time $t - \tau_\alpha^+$ when the source was at E_α^+. The point P lies on the intersection between two spherical phase surfaces which are both tangent to the Mach-cone and have their centres at E_β^- and E_β^+. Figure 3 is for the supercompressional motion ($M_\alpha > 1$).

The evaluation of $S_c(r, t)$ on the Mach-cone is given in the Appendix.

Consider, for example, a source with a unit-step time-dependence of the form $Q(t) = H(t - T)$. Equation (2.21) then shows that

$$S_{Lc}(r, t) = H(t - T) \int_T^t \frac{1}{D(t')} \delta\left(t - t' - \frac{D}{c}\right) dt' . \tag{2.24}$$

From Eqs. (2.22) and (2.23), we find

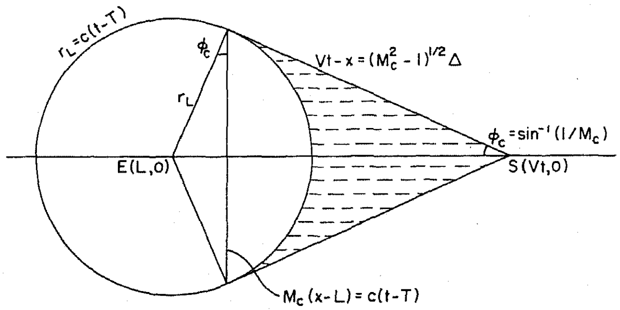

Fig. 4. The function Λ_{Lc} assumes value 1 in the shaded region bounded by the Mach-cone and the sphere and $\Lambda_{Lc}\equiv 0$ outside this region.

$$t-T-\tau_c^{\pm}=\frac{1}{c(1-M_c^2)}[c(t-T)-M_c(x-L)$$

$$\mp\{[c(t-T)-M_c(x-L)]^2-(1-M_c^2)[c^2(t-T)^2-r_L^2]\}^{1/2}], \tag{2.25}$$

where

$$r_L=[(x-L)^2+\Delta^2]^{1/2}, \qquad L=VT. \tag{2.26}$$

To evaluate the integral in Eq. (2.24), we look for the roots of the equation

$$t-t'-\frac{1}{c}D(t')=0 \tag{2.27}$$

which satisfy the condition $T<t'<t$. From Eq. (2.25) we note that the root $t'=t-\tau_c^+$ satisfies this condition in the following three cases:

I. $0\leq M_c\leq 1$ and $r_L<c(t-T)$.

II. $M_c>1$, $M_c(x-L)<c(t-T)$, and $r_L<c(t-T)$.

III. $M_c>1$, $M_c(x-L)\geq c(t-T)$, and $(Vt-x)\geq N_c\Delta$, where $N_c=\sqrt{(M_c^2-1)}$.

For $M_c>1$, the root $t'=t-\tau_c^-$ satisfies the condition $T<t'<t$ in the following two cases:

I. $M_c(x-L)\geq c(t-T)$ and $Vt-x=N_c\Delta$.

II. $M_c(x-L)\geq c(t-T)$, $Vt-x>N_c\Delta$, and $r_L>c(t-T)$.

Evaluating the integral (2.24), we find [cf., Eq. (2.20)]

$$S_{Lc}(r,t)=\frac{1}{R_c}\left[H\left(t-T-\frac{1}{c}r_L\right)+2\Lambda_{Lc}\right], \tag{2.28}$$

where $\Lambda_{Lc}=1$ inside the conical region (shaded in Fig. 4)

$$r_L>c(t-T), \qquad VT-x>N_c\Delta, \qquad M_c(x-L)>c(t-T), \tag{2.29}$$

and $\Lambda_{Lc}=0$ outside the region. Of course, $\Lambda_{Lc}\equiv 0$ if $M_c\leq 1$. We may write

$$\Lambda_{Lc}=H[r_L-c(t-T)]H[Vt-x-N_c\Delta]H[M_c(x-L)-c(t-T)]. \tag{2.30}$$

Equation (2.17) yields, for $Q(t)=H(t-T)$,

$$\ddot{\vec{G}}_{(T)}=\frac{\vec{I}}{4\pi\mu}\ddot{S}_{L\beta}-\frac{1}{4\pi\rho}\nabla\nabla(S_{L\beta}-S_{L\alpha}), \tag{2.31}$$

with S_{Lc} given by Eq. (2.28).

3. *Supershear Dipolar Sources That Start and Stop*

So far we have been dealing with the Green's tensor which yields the field due to a concentrated force. We show here how the field due to a point dipolar source, moving in the positive x-direction with a uniform velocity V and represented by the moment tensor $\vec{M}$, can be obtained. The equation of motion can be expressed in the form

$$\alpha^2 \operatorname{grad}\operatorname{div}\boldsymbol{u}-\beta^2 \operatorname{curl}\operatorname{curl}\boldsymbol{u}-\frac{\partial^2\boldsymbol{u}}{\partial t^2}=\frac{Q(t)}{\rho}\vec{M}\cdot\nabla\delta(\boldsymbol{r}-\boldsymbol{r}_0), \tag{3.1}$$

where

$$\delta(\boldsymbol{r}-\boldsymbol{r}_0)=\delta(x-Vt)\delta(y)\delta(z).$$

As in section 2, we decompose the displacement field and the source term into their irrotational and solenoidal parts in the form

$$\boldsymbol{u}=\operatorname{grad}\Phi-\operatorname{curl}\operatorname{curl}\boldsymbol{\Psi}, \tag{3.2}$$

$$-\vec{M}\cdot\nabla\delta(\boldsymbol{r}-\boldsymbol{r}_0)=\operatorname{grad}\Phi_0-\operatorname{curl}\operatorname{curl}\boldsymbol{\Psi}_0. \tag{3.3}$$

However

$$\begin{aligned}-\vec{M}\cdot\nabla\delta(\boldsymbol{r}-\boldsymbol{r}_0)&=\vec{M}\cdot\nabla\nabla^2\left(\frac{1}{4\pi D}\right)\\&=\frac{1}{4\pi}\nabla^2\left(\vec{M}\cdot\nabla\frac{1}{D}\right)\\&=\frac{1}{4\pi}\operatorname{grad}\operatorname{div}\left(\vec{M}\cdot\nabla\frac{1}{D}\right)\\&\quad-\frac{1}{4\pi}\operatorname{curl}\operatorname{curl}\left(\vec{M}\cdot\nabla\frac{1}{D}\right),\end{aligned} \tag{3.4}$$

assuming that $\vec{M}$ is a constant tensor. As before, $\boldsymbol{D}$ is the source-observer separation:

$$D(\boldsymbol{r},t)=[(x-Vt)^2+y^2+z^2]^{1/2}. \tag{3.5}$$

We thus have

$$\Phi_0=\frac{1}{4\pi}\operatorname{div}\left(\vec{M}\cdot\nabla\frac{1}{D}\right)=\frac{1}{4\pi}\vec{M}:\nabla\nabla\frac{1}{D}, \tag{3.6}$$

$$\boldsymbol{\Psi}_0=\frac{1}{4\pi}\vec{M}\cdot\nabla\frac{1}{D}. \tag{3.7}$$

The substitution of Eqs. (3.2) and (3.3) into the equation of motion (3.1) reveals that the potentials Φ and $\boldsymbol{\Psi}$ satisfy the wave equations

$$\alpha^2\nabla^2\Phi-\frac{\partial^2\Phi}{\partial t^2}=-\frac{Q(t)}{\rho}\Phi_0, \tag{3.8}$$

$$\beta^2\nabla^2\boldsymbol{\Psi}-\frac{\partial^2\boldsymbol{\Psi}}{\partial t^2}=-\frac{Q(t)}{\rho}\boldsymbol{\Psi}_0. \tag{3.9}$$

Writing

$$\Phi=-\vec{M}:\nabla\nabla F_\alpha, \qquad \boldsymbol{\Psi}=-\vec{M}\cdot\nabla F_\beta, \tag{3.10}$$

Eqs. (3.6) to (3.9) show that $F_{\alpha,\beta}$ satisfy Eq. (2.4). Knowing $F_{\alpha,\beta}$, Eq. (3.10) renders the potentials Φ and $\boldsymbol{\Psi}$ and then Eq. (3.2) yields the displacement field. A little algebra leads to the relation

$$\boldsymbol{u}=-\vec{M}:\nabla[\nabla\nabla(F_\alpha-F_\beta)+\nabla^2(F_\beta\vec{I})]. \tag{3.11}$$

The corresponding expression for the acceleration is

$$\begin{aligned}\ddot{\boldsymbol{u}}&=-\vec{M}:\nabla[\nabla\nabla(\ddot{F}_\alpha-\ddot{F}_\beta)+\nabla^2(\ddot{F}_\beta\vec{I})]\\&=-\vec{M}:\nabla\left[\frac{1}{4\pi\rho}\nabla\nabla(S_\alpha-S_\beta)+\frac{\vec{I}}{4\pi\mu}\ddot{S}_\beta\right],\end{aligned} \tag{3.12}$$

where

$$S_c=4\pi\rho c^2\nabla^2F_c, \qquad (c=\alpha,\beta). \tag{3.13}$$

The explicit expression for S_c for the cases $M_c \lesseqgtr 1$ are given in Eq. (2.22).

Equations (3.6) and (3.7) are very general. These yield the source potentials Φ_0 and $\boldsymbol{\Psi}_0$ if the moment tensor $\vec{M}$ is known. Table 1 gives the source potentials for various dipolar sources. In obtaining these potentials, we have made use of the following relations:

$$\nabla\frac{1}{D}=-\frac{\boldsymbol{D}}{D^3} \tag{3.14}$$

$$\nabla\nabla\frac{1}{D}=-\frac{4\pi}{3}\vec{I}\delta(\boldsymbol{r}-\boldsymbol{r}_0)+\frac{1}{D^5}(3\boldsymbol{D}\boldsymbol{D}-D^2\vec{I}), \tag{3.15}$$

where $\boldsymbol{D}=D\nabla D$. The expressions for the potentials given in Table 1 must be multiplied by $M_0/4\pi$, where M_0 is the seismic moment of the source.

For a point shear dislocation with normal $\boldsymbol{n}$ and slip-direction $\boldsymbol{e}$ ($\boldsymbol{e}\cdot\boldsymbol{n}=0$)

Table 1. The compressional and shear potentials for various dipolar sources.

Source	Compressional potential (Φ_0)
Centre of compression	$-4\pi\delta(r-r_0)$
Dipole in direction a	$\frac{1}{D^5}[3(a\cdot D)^2-D^2]-\frac{4\pi}{3}\delta(r-r_0)$
Single-couple (a, v)	$\frac{3}{D^5}(a\cdot D)(v\cdot D)$
Double-couple (a, v)	$\frac{6}{D^5}(a\cdot D)(v\cdot D)$
Torque $(a\times v)$	0
Tensile dislocation	$\frac{2}{D^5}[3(v\cdot D)^2-D^2]-4\pi\frac{\lambda+\frac{2}{3}\mu}{\mu}\delta(r-r_0)$

Source	Shear potential (Ψ_0)
Centre of compression	0
Dipole in direction a	$-\frac{1}{D^3}a(a\cdot D)$
Single-couple (a, v)	$-\frac{1}{D^3}a(v\cdot D)$
Double-couple (a, v)	$-\frac{1}{D^3}[a(v\cdot D)+v(a\cdot D)]$
Torque $(a\times v)$	$-\frac{1}{D^3}[a(v\cdot D)-v(a\cdot D)]$
Tensile dislocation	$-\frac{2}{D^3}v(v\cdot D)$

See Eq. (3.3) for definition. All expressions must be multiplied by $M_0/4\pi$. For a dislocation source.
$M_0=\mu\times$ magnitude of the slip $\times$ fault-area.

$$\vec{M}=M_0(en+ne)\,. \tag{3.16}$$

Assuming $Q(t)=H(t-T)$, Eqs. (3.12) and (3.16) yield

$$\ddot{u}_{(T)}=\frac{M_0}{2\pi\rho}en\colon \nabla\nabla\nabla(S_{L\beta}-S_{L\alpha})-\frac{M_0}{4\pi\mu}\{(e\cdot\nabla\ddot{S}_{L\beta})n+(n\cdot\nabla\ddot{S}_{L\beta})e\}\,, \tag{3.17}$$

where S_{Lc} is given in Eq. (2.28).

We now set up a fixed right-handed cartesian coordinate system with x-axis parallel to the direction of motion such that the dislocation plane coincides with the

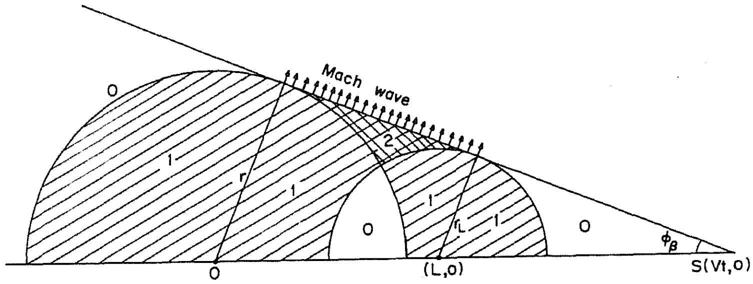

Fig. 5. The functions $H(t-r/\beta)-H(t-r_L/\beta)+2\Lambda_{0\beta}-2\Lambda_{L\beta}$ assumes the values 0, 1, or 2 depending upon the location of the observer.

xy-plane (Fig. 5). This is known as the fault coordinate system. Let the source be at the point $(0, y', 0)$ at time $t=0$. Then all of our previous results hold with

$$\Delta^2=(y-y')^2+z^2 .$$

We assume that

$$e=\cos\lambda e_x-\sin\lambda e_y , \qquad n=-e_z , \tag{3.18}$$

where λ denotes the slip-angle. Equation (3.17) now becomes

$$\ddot{u}_{(T)}=\frac{M_0}{2\pi\rho}\left[\left(\sin\lambda\frac{\partial}{\partial y}-\cos\lambda\frac{\partial}{\partial x}\right)\frac{\partial}{\partial z}\right]\nabla(S_{L\beta}-S_{L\alpha})$$
$$+\frac{M_0}{4\pi\mu}\left[\left(\cos\lambda\frac{\partial}{\partial x}-\sin\lambda\frac{\partial}{\partial y}\right)\ddot{S}_{L\beta}e_z+\frac{\partial\ddot{S}_{L\beta}}{\partial z}(\cos\lambda e_x-\sin\lambda e_y)\right]. \tag{3.19}$$

The choice of the source time-function

$$Q(t)=Q_L(t)\equiv Q_0(T)[H(t)-H(t-T)] \tag{3.20}$$

simulates a source of finite length L and propagation time $T=L/V$. $Q_0(T)$ is a dimensionless normalization factor that will henceforth be suppressed. In the limit $T\to 0$ $(L\to 0)$, we assume that $Q_0(T)\to T_0/T$, so that $Q_L(t)\to T_0\delta(t)$. As $V\to 0$, $Q_L(t)\to Q_0(T)H(t)$.

The acceleration for $Q_L(t)$ may be expressed in the form

$$\ddot{u}_L=\ddot{u}_{(0)}-\ddot{u}_{(T)} , \tag{3.21}$$

where $\ddot{u}_{(0)}$ corresponding to $Q(t)=H(t)$ is obtained simply on putting $T=0$ in Eq. (3.19). The field thus consists of a starting phase $\ddot{u}_{(0)}$ and a stopping phase $\ddot{u}_{(T)}$, having opposite polarities.

Equations (2.28), (3.19), and (3.21) yield the following expressions for the S-wave accelerations in the x-, y-, and z-directions.

3.1 Strike-slip ($\lambda=0$)

$$\ddot{u}_{LSx}=-\frac{M_0}{2\pi\rho}\left(\frac{\partial^2}{\partial x^2}-\frac{1}{2\beta^2}\frac{\partial^2}{\partial t^2}\right)\frac{\partial}{\partial z}\left[\frac{1}{R_\beta}\Omega_L(r,t)\right], \tag{3.22}$$

$$\ddot{u}_{LSy}=-\frac{M_0}{2\pi\rho}\frac{\partial^3}{\partial x\partial y\partial z}\left[\frac{1}{R_\beta}\Omega_L(r,t)\right], \tag{3.23}$$

$$\ddot{u}_{LSz}=-\frac{M_0}{2\pi\rho}\left(\frac{\partial^2}{\partial z^2}-\frac{1}{2\beta^2}\frac{\partial^2}{\partial t^2}\right)\frac{\partial}{\partial x}\left[\frac{1}{R_\beta}\Omega_L(r,t)\right], \tag{3.24}$$

where

$$\Omega_L(r,t)=H\left(t-\frac{r}{\beta}\right)-H\left(t-T-\frac{r_L}{\beta}\right)+2(\Lambda_{0\beta}-\Lambda_{L\beta}),$$

$$\Lambda_{0\beta}=H(r-\beta t)H(Vt-x-N_\beta\Delta)H(M_\beta x-\beta t), \tag{3.25}$$

and $\Lambda_{L\beta}$ is defined in Eq. (2.30).

3.2 Dip-slip ($\lambda=90°$)

$$\ddot{u}_{LSx}=\frac{M_0}{2\pi\rho}\frac{\partial^3}{\partial x\partial y\partial z}\left[\frac{1}{R_\beta}\Omega_L(r,t)\right], \tag{3.26}$$

$$\ddot{u}_{LSy}=\frac{M_0}{2\pi\rho}\left(\frac{\partial^2}{\partial y^2}-\frac{1}{2\beta^2}\frac{\partial^2}{\partial t^2}\right)\frac{\partial}{\partial z}\left[\frac{1}{R_\beta}\Omega_L(r,t)\right], \tag{3.27}$$

$$\ddot{u}_{LSz}=\frac{M_0}{2\pi\rho}\left(\frac{\partial^2}{\partial z^2}-\frac{1}{2\beta^2}\frac{\partial^2}{\partial t^2}\right)\frac{\partial}{\partial y}\left[\frac{1}{R_\beta}\Omega_L(r,t)\right]. \tag{3.28}$$

Similar expressions for the P-wave accelerations can be obtained without any difficulty.

The function $\Omega_L(r, t)$ assumes the values 0, 1, or 2 depending upon the location of the observer (Fig. 6). Differentiation of $\Omega_L(r, t)$ will result in the delta function and its first and second derivatives. For the Mach-wave, we have

$$\Omega_L(r,t)=H(Vt-x-N_\beta\Delta)\left[H\left(x-\frac{\Delta}{N_\beta}\right)-H\left(x-L-\frac{\Delta}{N_\beta}\right)\right], \tag{3.29}$$

and the differentiations implied in Eqs. (3.22) to (3.28) will yield $H(Vt-x-N_\beta\Delta)$, $\delta(Vt-x-N_\beta\Delta)$, $\delta'(Vt-x-N_\beta\Delta)$, and $\delta''(Vt-x-N_\beta\Delta)$.

In all, we have the following arrivals:

3.3 P-wave arrivals

Starting phase: $t=r/\alpha$.

Stopping phase: $t=T+r_L/\alpha$.

Mach-wave: $t=(x+N_\alpha\Delta)/\alpha$.

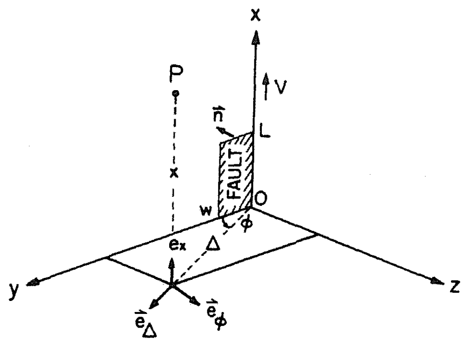

Fig. 6. Circular cylinder coordinates associated with the stationary-phase approximation of the acceleration-field.

3.4 S-wave arrivals
Starting phase: $t=r/\beta$.
Stopping phase: $t=T+r_L/\beta$.
Mach-wave: $t=(x+N_\beta\Delta)/\beta$.

The Mach-wave arrives first. It is followed by the starting phase or the stopping phase depending upon the location. The points at which the starting phase and the stopping phase arrive simultaneously lie on one branch of the hyperbola $r-r_L=cT$. At any given time t, the points which receive the Mach-wave lie on the conical surface (Fig. 6)

$$Vt-x=N_c\Delta\,,\qquad \frac{\Delta}{N_c}<x<\frac{\Delta}{N_c}+L. \tag{3.30}$$

4. *Approximation of the Acceleration-Field in the Near-Fault Region*

Equation (2.19) can be written in the form

$$\vec{G}(r,\omega)=\frac{\vec{I}}{4\pi\mu}K_\beta+\frac{1}{4\pi\rho\omega^2}\nabla\nabla(K_\beta-K_\alpha)\,, \tag{4.1}$$

where

$$K_c=\int_{-\infty}^{\infty}\frac{Q(t')}{D(t')}\mathrm{e}^{-i\omega(t'+D/c)}\mathrm{d}t'\,. \tag{4.2}$$

We recall Kelvin's formula

$$\int_{-\infty}^{\infty}B(s)\mathrm{e}^{-i\omega b(s)}\mathrm{d}s=\left[\frac{2\pi}{\omega\,|b''(s_0)|}\right]^{1/2}B(s_0)\mathrm{e}^{-i\omega b(s_0)-(\pi i/4)\operatorname{sgn}b''(s_0)}+O(\omega^{-1})\,, \tag{4.3}$$

where $b'(s_0)=0$. Assuming $M_\alpha<1<M_\beta$, we obtain

$$K_\alpha=\left(\frac{2\pi}{\omega V\Delta}\right)^{1/2}(1-M_\alpha^2)^{-1/4}Q(t'_\alpha)\exp\left[-i\omega\frac{x}{V}-|\omega|\frac{\Delta}{V}\sqrt{1-M_\alpha^2}-\frac{\pi i}{2}\right]+O(\omega^{-1}), \tag{4.4}$$

$$K_\beta=\left(\frac{2\pi}{\omega V\Delta}\right)^{1/2}(M_\beta^2-1)^{-1/4}Q(t'_\beta)\exp\left[-i\frac{\omega}{V}(x+\Delta\sqrt{M_\beta^2-1})-\frac{\pi i}{4}\right]+O(\omega^{-1}) \tag{4.5}$$

where

$$t'_\alpha=\frac{1}{V}[x-i\Delta(1-M_\alpha^2)^{-1/2}], \qquad t'_\beta=\frac{1}{V}[x-\Delta(M_\beta^2-1)^{-1/2}]. \tag{4.6}$$

Because of the exponential decay, K_α can be ignored. Thus, assuming $|\omega|$ large, we have the approximation

$$\begin{aligned}\vec{\vec{G}}(r,\omega)=&\frac{\omega^{-1/2}}{4\pi\mu}\left(\frac{2\pi}{V\Delta i}\right)^{1/2}\frac{1}{M_\beta^2\sqrt{N_\beta}}Q(t'_\beta)\exp\left[-\frac{i\omega}{V}(x+N_\beta\Delta)\right]\\ &\times[N_\beta^2 e_x e_x-N_\beta(e_x e_\Delta+e_\Delta e_x)+M_\beta^2 e_\varphi e_\varphi+e_\Delta e_\Delta],\end{aligned} \tag{4.7}$$

where

$$\Delta e_\Delta=ye_y+ze_z, \qquad \Delta e_\varphi=-ze_y+ye_z. \tag{4.8}$$

Under the same approximation

$$\begin{aligned}\nabla\vec{\vec{G}}(r,\omega)=&-\frac{\omega^{1/2}}{4\pi\mu}\left(\frac{2\pi i}{V^3\Delta}\right)^{1/2}\frac{Q(t'_\beta)}{M_\beta^2\sqrt{N_\beta}}\exp\left[-i\frac{\omega}{V}(x+N_\beta\Delta)\right]\\ &\times[N_\beta^2 e_x e_x e_x+N_\beta e_\Delta e_\Delta e_\Delta-N_\beta(e_x e_x e_\Delta+e_x e_\Delta e_x-N_\beta^2 e_\Delta e_x e_x)\\ &+e_x e_\Delta e_\Delta-N_\beta^2(e_\Delta e_x e_\Delta+e_\Delta e_\Delta e_x)+M_\beta^2(e_x e_\varphi e_\varphi+N_\beta e_\Delta e_\varphi e_\varphi)].\end{aligned} \tag{4.9}$$

Note that components of $\vec{\vec{G}}$ and $\nabla\vec{\vec{G}}$ are given here, for the sake of convenience, in a cylindrical coordinate system (x, Δ, ϕ) as shown in Fig. 6.

The acceleration field due to a displacement dislocation can now be calculated through the relation

$$\ddot{u}=-\vec{\vec{M}}:\nabla\ddot{\vec{\vec{G}}}. \tag{4.10}$$

Equations (3.16), (4.9), and (4.10) yield

$$\ddot{u}(r,\omega)=\left[\frac{\omega^{5/2}}{4\pi\mu}\left(\frac{2\pi i}{V^3\Delta}\right)^{1/2}Q(t'_\beta)\exp\left[-i\frac{\omega}{V}(x+N_\beta\Delta)\right]\right]M_0\boldsymbol{J}, \tag{4.11}$$

in which the vector $\boldsymbol{J}$ depends upon the source.

For a strike-slip dislocation,

$$J=\frac{1}{M_\beta^2\sqrt{N_\beta}}\left[N_\beta(2-M_\beta^2)\frac{z}{\Delta}e_x-(2-M_\beta^2)\frac{z}{\Delta}e_\Delta-M_\beta^2\frac{y}{\Delta}e_\varphi\right], \tag{4.12}$$

and, for a dip-slip dislocation,

$$J=\frac{\sqrt{N_\beta}}{M_\beta^2}\left[-2N_\beta\frac{yz}{\Delta^2}e_x+2\frac{yz}{\Delta^2}e_\Delta+M_\beta^2\frac{y^2-z^2}{\Delta^2}e_\varphi\right]. \tag{4.13}$$

Assuming $Q(t'_\beta)=1$ and applying the inverse Fourier transform to Eq. (4.11), we obtain

$$\ddot{u}(r,t)=\frac{M_0}{4\pi\mu}\left(\frac{2}{\pi V^3\Delta}\right)^{1/2}J\int_0^\infty\omega^{5/2}\cos(\omega t^*+\pi/4)\mathrm{e}^{-p\omega}\mathrm{d}\omega\,, \tag{4.14}$$

where

$$t^*=t-\frac{1}{V}(x+N_\beta\Delta)\,,\qquad p=\frac{\Delta}{2\beta Q_\beta}\,,\qquad Q_\beta=\text{quality factor}\,. \tag{4.15}$$

The factor $\mathrm{e}^{-p\omega}$ has been introduced to take into account the anelasticity of the medium. Using the integral

$$\int_0^\infty\omega^{q-1}\mathrm{e}^{-p\omega}\cos(\omega t^*+\delta)\mathrm{d}\omega=\Gamma(q)\frac{\cos(q\chi+\delta)}{(p^2+t^{*2})^{q/2}}\,, \tag{4.16}$$

$$[\chi=\tan^{-1}(t^*/p)]$$

Eq. (4.14) yields

$$\ddot{u}(r,t)=\left[\frac{15}{16\pi\mu V}\left(\frac{1}{2V\Delta}\right)^{1/2}\frac{\cos\left(\frac{7}{2}\chi+\frac{\pi}{4}\right)}{(p^2+t^{*2})^{7/4}}\right]M_0J\,. \tag{4.17}$$

Since the peak of the Mach-wave arrives at $t^*=0$, the peak of the acceleration signal will have the value

$$\ddot{u}(r,t^*=0)=\left[\frac{15Q_\beta^{7/2}}{2\sqrt{2\pi}\rho M_\beta^{3/2}\Delta^4}\right]M_0J\qquad(\Delta\neq0,\ M_\beta>1)\,. \tag{4.18}$$

In Eq. (4.18), the point of observation must avoid the source-location at the intersection of the Mach-front and the x-axis. Hence it is not valid at $\Delta=0$. Away from this axis, the Mach peak acceleration diminishes as the inverse 4th power of the normal distance from the line of motion and increases with the (7/2)th power of the dimensionless shear quality factor of the anelastic medium. In particular, for a shallow source ($y'\approx0$), the Mach peak acceleration decreases as the inverse fourth power of the normal horizontal distance from the fault. Thus, the present approximation serves to show that, in effect, the major contribution to the acceleration field, in the near-fault zone arises from the Mach-wave and not from either the starting or the stopping phases.

Note that there is no conflict between the validity of Eq. (4.3) for high frequencies and the application of Eq. (4.16) over the entire frequency range: the amplitude of the integrand in Eq. (4.16) peaks at $\omega_0 = 5\beta Q_\beta/\Delta$, and the condition $\omega_0 \gg 1$ is valid in the near-fault zone in most earth materials.

The final result for the peak acceleration at the time of arrival of the Mach-wave, as given in Eq. (4.18), depends on the medium's unelasticity. This must be so since in a perfectly elastic medium, the arrival of the Mach-wave is marked by infinite amplitude which is not physical. Our result here is similar to the response of a linear dissipative system at resonance.

5. *Conclusions and Discussion*

Our model and results differ from those of the previous studies in a number of ways:

(1) We have derived, in closed form, the Green's tensor and its gradient for arbitrary shear and compressional Mach-numbers.

(2) In contradistinction to the common kinematic dislocation model with a propagating Heaviside step-function, we have used a propagating delta function which is proportional to the slip-velocity [i.e., the time-derivative of $H(t-x/V)$]. Thus, while the common kinematic model does not exhibit any displacement singularity higher than a step function, our solutions predict the arrivals of displacement step and delta functions. Our model predicts the arrivals of sharp acceleration peaks, already in the subshear region.

(3) We have shown that the Mach-wave plays a dominant role in the acceleration-field of the near-fault zone. In part II of this paper, we shall present numerical results that emphasize the dependence of the acceleration-field on the Mach-number in the near-fault zone.

S.J.S. wishes to thank the Department of Applied Mathematics of the Weizmann Institute of Science for a Visiting Fellowship during Feb.–May 1986 and the University Grants Commission, New Delhi, for a National Fellowship.

APPENDIX

The Supersonic Green's Function on the Mach-Cone

We have shown in Eq. (2.22) that, for $M_c > 1$,

$$S_c(r, t) = \frac{1}{R_c}\left[Q\left(t - \frac{R_c^+}{c}\right) + Q\left(t - \frac{R_c^-}{c}\right)\right], \tag{A.1}$$

for points inside the Mach-cone and $S_c(r, t) \equiv 0$ for points outside the Mach-cone. We now wish to determine $S_c(r, t)$ for points on the Mach-cone

$$R_c = 0\,, \qquad x < Vt\,, \qquad Vt - x = (M_c^2 - 1)^{1/2}\Delta\,. \tag{A.2}$$

Returning to Eq. (2.22), we note that $D(t') = 0$ has a double root at $\tau = \hat{\tau} = \hat{R}/c$, where

$$\hat{R} = M_c(Vt - x)/(M_c^2 - 1)\,. \tag{A.3}$$

Now, the Dirac delta function is known to have the property

$$\delta[s(\tau)] = -\frac{\delta'(\tau - \hat{\tau})}{|s''(\hat{\tau})|}\,, \tag{A.4}$$

where $\hat{\tau}$ is a double root of $s(\tau) = 0$. The explicit form of this equation is

$$(1 - M_c^2)V^2 t'^2 + 2V(M_c^2 x - Vt)t' + V^2 t^2 - M_c^2 r^2 = 0\,, \tag{A.5}$$

where $M_c = V/c$ is the Mach-number and

$$r^2 = x^2 + \Delta^2\,.$$

Putting $\tau = t - t'$, Eq. (A.5) becomes

$$c^2(1 - M^2)\tau^2 - 2V(x - Vt)\tau - [(x - Vt)^2 + \Delta^2] = 0\,. \tag{A.6}$$

For $M = 1$, Eq. (A.6) has a single root at

$$\tau_0 = \frac{(ct - x)^2 + \Delta^2}{2c(ct - x)}\,. \tag{A.7}$$

Evaluating the integral in Eq. (2.22), we have, for a point on the Mach-cone,

$$S_c(r, t) = \frac{1}{M(Vt - x)}Q\left(t - \frac{\hat{R}}{c}\right) + \frac{1}{c}Q'\left(t - \frac{\hat{R}}{c}\right), \tag{A.8}$$

where we have used the result

$$\int_{-\infty}^{\infty} f(x)\delta'(x - x_0)\mathrm{d}x = -f'(x_0)\,. \tag{A.9}$$

List of Symbols

$c = \alpha$ or β, $k_c = \omega/c$, $M_c = V/c$, $N_c = (M_c^2 - 1)^{1/2}$

$\Delta = (y^2 + z^2)^{1/2}$

$r = (x^2 + \Delta^2)^{1/2}$, $r_L = [(x - L)^2 + \Delta^2]^{1/2}$

$D(t) = [(x - Vt)^2 + \Delta^2]^{1/2}$

$R = [(x - Vt)^2 + (1 - M_c^2)\Delta^2]^{1/2}$

$R_c = [(x - Vt)^2 + (1 - M_c^2)\Delta^2]^{1/2}$

$\quad = R_c^+(1 - M_c\cos\psi_c^+)$

$\quad = R_c^-(M_c\cos\psi_c^- - 1)$

$$R_{\pm}=\frac{1}{1-M_c^2}[M_c(x-Vt)\pm R]$$

$$R_c^{\pm}=\frac{1}{1-M_c^2}[M_c(x-Vt)\pm R_c]$$

$$R_0=R_c^0=\frac{(ct-x)^2+\Delta^2}{2(ct-x)}$$

$$\cos\psi_{\pm}=M_c+\frac{x-Vt}{R_{\pm}}$$

$$\cos\psi_c^{\pm}=M_c+\frac{x-Vt}{R_c^{\pm}}$$

$$\tau_{\pm}=t-t_{\pm}=\frac{1}{c}R_{\pm}$$

$$\tau_c^{\pm}=t-t_c^{\pm}=\frac{1}{c}R_c^{\pm}$$

$$\tau_0=t-t_0=\tau_c^0=\frac{1}{c}R_c^0$$

$\delta(t-t')=$ Dirac delta function
$\delta(\boldsymbol{r}-\boldsymbol{r}')=\delta(x-x')\delta(y-y')\delta(z-z')$
$H(t-t')=$ Unit step function

$$\Omega_L(\boldsymbol{r},t)=H\left(t-\frac{r}{\beta}\right)-H\left(t-T-\frac{r_L}{\beta}\right)+2(\Lambda_{0\beta}-\Lambda_{L\beta})$$

$\Lambda_{0\beta}=H(r-\beta t)H(Vt-x-N_\beta\Delta)H(M_{\beta x}-\beta t)$
$\Lambda_{L\beta}=H[r_L-\beta(t-T)]H[Vt-x-N_\beta\Delta]H[M_\beta(x-L)-\beta(t-T)]$
$Q_\beta=$ shear-waves quality factor
$Q(t)=$ source's time-function

Conventions

$$\boldsymbol{en}:\boldsymbol{ab}=(\boldsymbol{e}\cdot\boldsymbol{b})(\boldsymbol{n}\cdot\boldsymbol{a})$$

REFERENCES

ARCHULETA, R. J., A faulting model for the 1979 Imperial Valley earthquake, *J. Geophys. Res.*, **89**, 4559–4585, 1984.

BEN-MENAHEM, A., Radiation of seismic surface waves from finite moving sources, *Bull. Seismol. Soc. Am.*, **51**, 401–435, 1961.

BEN-MENAHEM, A. and S. J. SINGH, *Seismic Waves and Sources*, Springer-Verlag, New York, 1108 pp., 1981.

BURRIDGE, R., Admissible speeds for plane strain self similar shear cracks with friction but lacking cohesion, *Geophys. J. R. Astron. Soc.*, **35**, 439–456, 1973.

CLOUD, W. K. and V. PEREZ, Unusual accelerations recorded at Lima, Peru, *Bull. Seismol. Soc. Am.*, **61**, 633–640, 1971.

DAS, S. and K. AKI, Fault plane with barriers: A versatile earthquake model, *J. Geophys. Res.*, **82**, 5658–5670, 1977.

EASON, G., J. FULTON, and I. N. SNEDDON, The generation of waves in an infinite elastic solid by variable body forces, *Philos. Trans. R. Soc. London*, **A248**, 575–607, 1956.

ESHELBY, T. D., Uniformly moving dislocations, *Proc. Phys. Soc.*, **A62**, 307–314, 1949.

FRANK, F. C., On the equations of motion of crystal dislocations, *Proc. Phys. Soc.*, **A62**, 131–134, 1949.

MADARIAGA, R., High frequency radiation from dynamic earthquake fault models, *Ann. Geophys.*, **1**, 17–23, 1983.

MURRAY, G. F., Dislocation mechanism—The Parkfield 1966 accelerograms, *Bull. Seismol. Soc. Am.*, **63**, 1539–1555, 1973.

PAYTON, R. G., An application of the dynamic Betti-Rayleigh reciprocal theorem to moving-point loads in elastic media, *Q. Appl. Math.*, **21**, 299–313, 1963.

SAVAGE, J. C., Radiation from supersonic faulting, *Bull. Seismol. Soc. Am.*, **61**, 1009–1012, 1971.